Adaptive Fuzzy Fault-Tolerant Control for a Riser-Vessel System With Unknown Backlash

Zhijia Zhao, *Member, IEEE*, Yiming Liu, Ge Ma, Keum-Shik Hong, *Fellow, IEEE*, and Han-Xiong Li, *Fellow, IEEE*

***Abstract*—In this article, we propose a new adaptive fuzzy fault-tolerant control (FTC) for a three-dimensional riser-vessel system with unknown backlash nonlinearity. A model for the smooth inverse dynamics of the backlash is introduced; then, the control input is divided into an expected input and a compensation error. Considering the imprecision of system modeling and unknown external disturbances, we employ a fuzzy adaptive technology to achieve compensation. By incorporating the actuator fault term and backlash error, the adaptive FTC is developed to resolve loss faults in the actuator and compensate for the unknown backlash to some extent. The direct Lyapunov method is used to demonstrate the system's bounded stability. Finally, simulation results demonstrate the effectiveness of the derived scheme.**

***Index Terms*—Adaptive control, fault-tolerant control (FTC), fuzzy control, inverse backlash dynamics, riser-vessel system.**

I. Introduction

MARINE risers play a crucial role in deep water oil and gas development projects, as they are the main channels connecting offshore floating devices and submarine pipelines [1]. Risers face a series of complex technical problems in harsh marine environments. For example, there is a rise in pressure acting on the pipe as the depth increases. Concurrently, capricious ocean currents also pose a threat to pipe structures. Compared with rigid structures, flexible structures can make the riser lighter and more suitable for the seabed environment. However, deformation inevitably appears in flexible risers owing to complicated environments, vibrations, and unknown disturbances, which will affect the service life of risers and even lead to oil and gas leakage. Thus, efficient control technologies should be developed for flexible risers.

The riser model is a distributed parameter system (DPS) [2]. If the system is reduced to a finite-dimensional state space for control design, it may produce an adverse spillover effect. Fortunately, this problem can be addressed via boundary control (BC), and fewer sensors and actuators are required during execution [3], [4]. In recent years, significant progress has been made in the study of BC methods for flexible risers [5]. In [6], a new boundary iterative learning control strategy was proposed to compensate for external disturbances, input saturation, and output constraint of one-dimensional (1-D) flexible risers. To address parameter uncertainties and asymmetric nonlinear input dead zones in riser systems, a robust adaptive control was designed in [7]. In [8], an adaptive robust control method for three-dimensional (3-D) uncertain riser-vessel systems was developed. However, these previous studies were limited to the vibration suppression of 1-D or 3-D flexible riser systems, and the methods used are not applicable to 3-D riser-vessel systems with input backlash.

Backlash is among the common nonlinearities in industrial system mechanical actuators. It may be caused by gear clearance and friction of control valve components, among other causes. The backlash nonlinearity leads to an increase in system performance degradation and even to an unstable system. To address this problem, various approaches have been proposed. The backlash is resolved by a simple anti-backlash torsion torque and a virtual average motor model in [9]. In [10], a fuzzy backlash model was adopted to describe the uncertainty actuator backlash input nonlinearity. The best way to compensate for input backlash is to use an inverse to eliminate it [11]. The authors introduced a smooth inverse function to model the backlash and incorporated it into the controller design using the backstepping technique in [12]. Note that the literature was confined to stabilizing finite-dimensional systems with backlash, and these methodologies are not available for infinite-dimensional flexible systems. Recently, significant advances in tracking the backlash of flexible systems were documented in [13]. In [14], the backlash was formulated as a linear input and the addition of interference-like terms; then, a new auxiliary term was introduced to compensate for the influence of backlash. In [15], a new control strategy was proposed by introducing adaptive

Manuscript received 7 November 2022; accepted 5 June 2023. Date of publication 29 June 2023; date of current version 18 September 2023. This work was supported in part by the National Natural Science Foundation of China under Grant 62273112; in part by the Science and Technology Planning Project of Guangzhou City under Grant 202201010758 and Grant 2023A03J0120; in part by the Open Research Fund from the Guangdong Laboratory of Artificial Intelligence and Digital Economy [Shenzhen (SZ)] under Grant GML-KF-22-27; and in part by the National Research Foundation of Korea under the Ministry of Science and ICT, South Korea, under Grant RS-2023-00207954. This article was recommended by Associate Editor Z. Peng. *(Corresponding author: Ge Ma.)*

Zhijia Zhao, Yiming Liu, and Ge Ma are with the School of Mechanical and Electrical Engineering, Guangzhou University, Guangzhou 510006, China (e-mail: zhjzhaoscut@163.com; 2112107115@e.gzhu.edu.cn; m_ge@gzhu.edu.cn).

Keum-Shik Hong is with the School of Mechanical Engineering, Pusan National University, Busan 46241, Republic of Korea (e-mail: kshong@pusan.ac.kr).

Han-Xiong Li is with the Department of Advanced Design and Systems Engineering, City University of Hong Kong, Hong Kong (e-mail: mehxli@cityu.edu.hk).

Color versions of one or more figures in this article are available at https://doi.org/10.1109/TSMC.2023.3285653.

Digital Object Identifier 10.1109/TSMC.2023.3285653

inverse backlash dynamics to handle a flexible riser system with input backlash. However, the aforementioned studies handled the backlash nonlinearity in flexible systems in the presence of known backlash parameters, and these approaches are ineffective in addressing the uncertainties of backlash slope. Moreover, the unsmooth backlash inverse dynamics in [15] and [16] may result in more chattering in the actuators. Although significant developments have been attained in disposing the backlash of flexible systems, no research has been reported on employing the smooth inverse backlash dynamics to eliminate the backlash in 3-D flexible riser systems, which is the motivation for the present study.

Uncertainties and actuator faults universally exist in controlled system and pose a significant challenge to the control design [17]. For actuator faults, an adaptive fault-tolerant control (FTC) for in-wheel motor drive electric vehicles via a reinforcement learning algorithm was proposed in [18]. In [19], an effective adaptive actuator fault compensation scheme was adopted for a class of parameter-strict-feedback MIMO nonlinear systems. In recent years, many researchers have been dedicated to developing a wide variety of control methods to address the uncertainties or actuator faults in flexible systems [20], [21]. In [22], considering the system uncertainty, an adaptive neural feedback control for nonlinear flexible DPSs was proposed. In [23], a robust adaptive control allocation algorithm with actuator fault compensation was presented for flexible string systems. Although successful solutions have been provided on the BC of flexible systems preceded by uncertainties or actuator faults, the control design for a 3-D flexible riser-vessel system with unknown backlash, actuator faults, and model uncertainties remains an open issue, which drives further research.

Motivated by this background, we intend to develop a new adaptive fuzzy FTC for a 3-D riser-vessel system with unknown backlash, actuator faults, and model uncertainties. The main contributions of the present study can be summarized as follows.

1) In contrast to previous studies [8], [24], [25], [26], the modeling uncertainties and external disturbances are incorporated into the unmodeled terms, and then a fuzzy-logic system (FLS) is utilized for approximation compensation.
2) The chattering issue caused by the unsmooth inverse is resolved by introducing smooth inverse backlash dynamics and an adaptive mapping operator.
3) An adaptive fuzzy FTC is established to address the actuator faults, compensate for the model uncertainties, eliminate the unknown backlash, and stabilize the vibration in 3-D flexible riser systems.

II. Problem Statement

A. System Model

Fig. 1 depicts a schematic of a 3-D flexible riser-vessel system, where *ODEF* represents the coordinate system. Here, μ, ω, and τ denote the independent time variable, space variable, and riser length, respectively; $d(\omega,\mu)$, $e(\omega,\mu)$, and $f(\omega,\mu)$ denote the vibrational deflection of the riser in

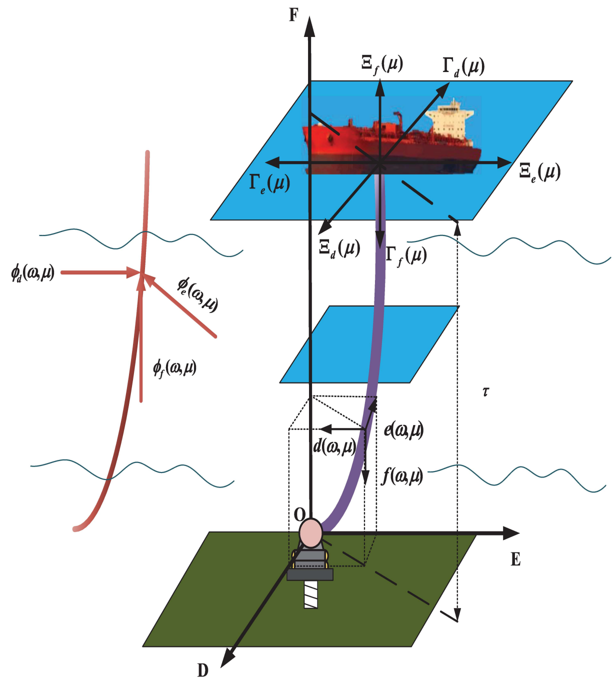

Fig. 1. Riser-vessel system.

the *DEF* directions; and $\Phi_d(\omega,\mu)$, $\Phi_e(\omega,\mu)$, and $\Phi_f(\omega,\mu)$ represent the distributed disturbances on the riser system in the *DEF* directions. The model uncertainties of the riser system are expressed as $\Theta_{fd}(\mu)$, $\Theta_{fe}(\mu)$, and $\Theta_{ff}(\mu)$; $\Gamma_d(\mu)$, $\Gamma_e(\mu)$, and $\Gamma_f(\mu)$ denote the extraneous disturbances that act upon the tip of the riser; and $\Xi_d(\mu)$, $\Xi_e(\mu)$, and $\Xi_f(\mu)$ are the BC inputs in the *DEF* directions. $\mathcal{R}$ represents a collection of real numbers. For simplicity, some symbols are defined as follows: $(*)=(*)(\omega,\mu)$, $(*)_\mu=\partial(*)/\partial\mu$, $(*)_\omega=\partial(*)/\partial\omega$, $(*)_{\omega\mu}=\partial^2(*)/\partial\omega\partial\mu$. $(*)_{\omega\omega}=\partial^2(*)/\partial\omega^2$, $(*)_{\omega\omega\omega}=\partial^3(*)/\partial\omega^3$, $(*)_{\omega\omega\omega\omega}=\partial^4(*)/\partial\omega^4$, $(*)_{\mu\mu}=\partial^2(*)/\partial\mu^2$, $(*)_0=(*)(0,\mu)$, $(*)_\tau=(*)(\tau,\mu)$, and $\tilde{*}=*-\hat{*}$ for $(\omega,\mu)\in[0,\tau]\times[0,+\infty)$.

First, we consider the system's dynamical model as follows [8]:

$$\varsigma d_{\mu\mu}=EA(f_{\omega\omega}d_\omega+d_{\omega\omega}f_\omega)+Td_{\omega\omega}+\frac{3}{2}EAd_\omega^2d_{\omega\omega}$$
$$-EId_{\omega\omega\omega\omega}+\frac{1}{2}EA\Big[d_{\omega\omega}e_\omega^2+2d_\omega e_\omega e_{\omega\omega}\Big]+\Phi_d \quad (1)$$

$$\varsigma e_{\mu\mu}=EA(f_{\omega\omega}e_\omega+e_{\omega\omega}f_\omega)+Te_{\omega\omega}+\frac{3}{2}EAe_\omega^2e_{\omega\omega}$$
$$-EIe_{\omega\omega\omega\omega}+\frac{1}{2}EA\Big[e_{\omega\omega}d_\omega^2+2e_\omega d_\omega d_{\omega\omega}\Big]+\Phi_e \quad (2)$$

$$\varsigma f_{\mu\mu}=EAd_\omega d_{\omega\omega}+EAe_\omega e_{\omega\omega}+EAf_{\omega\omega}+\Phi_f \quad (3)$$

with the following boundary conditions:

$$\Xi_d-md_{\tau\mu\mu}=-EId_{\tau\omega\omega\omega}+EAd_{\tau\omega}f_{\tau\omega}+Td_{\tau\omega}-\Gamma_d$$
$$+\frac{1}{2}EA\Big(d_{\tau\omega}e_{\tau\omega}^2+d_{\tau\omega}^3\Big)-\Theta_{fd} \quad (4)$$

$$\Xi_e-me_{\tau\mu\mu}=-EIe_{\tau\omega\omega\omega}+EAe_{\tau\omega}f_{\tau\omega}+Te_{\tau\omega}-\Gamma_e$$
$$+\frac{1}{2}EA\Big(e_{\tau\omega}d_{\tau\omega}^2+e_{\tau\omega}^3\Big)-\Theta_{fe} \quad (5)$$

$$\Xi_f-mf_{\tau\mu\mu}=\frac{1}{2}EAd_{\tau\omega}^2+\frac{1}{2}EAe_{\tau\omega}^2+EAf_{\tau\omega}-\Gamma_f$$
$$-\Theta_{ff} \quad (6)$$

$$d_{0\omega\omega}=e_{0\omega\omega}=f_{0\omega\omega}=0,\quad d_{\tau\omega\omega}=e_{\tau\omega\omega}=f_{\tau\omega\omega}=0 \quad (7)$$

where m represents the vessel mass, and the uniform mass per unit length, tension, axial stiffness, and bending stiffness of the flexible riser are expressed as ς, T, EA, and EI, respectively.

B. Actuator Fault and Input Backlash

In this study, we consider a riser-vessel system subject to the unknown backlash and actuator fault.

Then, the backlash expressions are presented as [27]

$$\Pi_j(\mu) = B\big(\varpi_j(\mu)\big) = \begin{cases} \varrho_j\big(\varpi_j - B_{rj}\big), & \text{if } \dot{\varpi}_j > 0 \text{ and } \Pi_j = \varrho_j\big(\varpi_j - B_{rj}\big) \\ \varrho_j\big(\varpi_j - B_{lj}\big), & \text{if } \dot{\varpi}_j < 0 \text{ and } \Pi_j = \varrho_j\big(\varpi_j - B_{lj}\big) \\ \Pi_j(\mu\_), & \text{otherwise} \end{cases} \tag{8}$$

where $\varrho_j \geq \varrho_{0j}$, $j = d, e, f$, denote the slope of the lines, with ϱ_{0j}, $j = d, e, f$, being small positive numbers. B_{rj} and B_{lj}, $j = d, e, f$ are constants greater than zero and less than zero, respectively; $\varpi_j(\mu)$, $j = d, e, f$, represent the expected control to be developed; $\Pi_j(\mu)$, $j = d, e, f$, describe the actual input affected by the backlash and $\Pi_j(\mu\_)$, $j = d, e, f$, show no change in $\Pi_j(\mu)$.

Remark 1: As opposed to previous studies [8], [24], [25], we consider the modeling uncertainties including the uncertainty of system parameters. For example, the deflection at the top of the riser will have a significant impact on the top tension of the marine riser [28]. In order to avoid designing the adaptive laws of multiple parameters [29], we propose a fuzzy compensation strategy. In addition, in previous studies [13], [15], the inverse backlash compensation control was investigated based on the assumption that the backlash slope is a known constant and the left and right "crossing" terms are symmetrical. However, the backlash parameters may be unknown in reality; therefore, a new compensation method is required for backlash compensation.

To avoid the chattering caused by the unsmooth inverse compensation operator, we introduce the following smooth backlash inverse dynamics [12]:

$$\varpi_j(\mu) = BI\big(\Pi_j\big) = \frac{1}{\varrho_j}\Pi_j + B_{rj}G_{rj}\big(\dot{\Pi}_j\big) + B_{lj}G_{lj}\big(\dot{\Pi}_j\big) \tag{9}$$

where $G_{rj}(\dot{\Pi}_j)$ and $G_{lj}(\dot{\Pi}_j)$, $j = d, e, f$, are defined as

$$G_{rj}\big(\dot{\Pi}_j\big) = \frac{e^{(P_j\dot{\Pi}_j)}}{e^{(P_j\dot{\Pi}_j)} + e^{(-P_j\dot{\Pi}_j)}} \tag{10}$$

$$G_{lj}\big(\dot{\Pi}_j\big) = \frac{e^{(-P_j\dot{\Pi}_j)}}{e^{(P_j\dot{\Pi}_j)} + e^{(-P_j\dot{\Pi}_j)}} \tag{11}$$

where P_j, $j = d, e, f$, are positive constants. The larger the P_j values are, the closer G_{rj} is to 1 and 0 when $\dot{\Pi}_j \to \infty$ and $\dot{\Pi}_j \to -\infty$, respectively. In contrast, G_{lj} is closer to 0 and 1 when $\dot{\Pi}_j \to \infty$ and $\dot{\Pi}_j \to -\infty$, respectively. Because both G_{rj} and G_{lj} are continuously differentiable, the chattering caused by the nonsmooth inverse indicator function can be settled.

To address the backlash parameter uncertainty, we rewrite (9) as follows:

$$\varpi_j(\mu) = \widehat{BI}\big(\Pi_{dj}(\mu)\big) = \frac{1}{\widehat{\varrho}_j}\big[\Pi_{dj}(\mu) + \widehat{\varrho_j B_{rj}}G_{rj}\big(\dot{\Pi}_{dj}\big) + \widehat{\varrho_j B_{lj}}G_{lj}\big(\dot{\Pi}_{dj}\big)\big] \tag{12}$$

where $\Pi_{dj}(\mu)$, $j = d, e, f$, represent the actual actuator inputs after compensation. $\widehat{\varrho}_j$, $\widehat{\varrho_j B_{rj}}$, and $\widehat{\varrho_j B_{lj}}$ denote the estimates of ϱ_j, $\varrho_j B_{rj}$, and $\varrho_j B_{lj}$, $j = d, e, f$, respectively.

Invoking (12), the expressions of $\Pi_{dj}(\mu)$ are given as

$$\Pi_{dj}(\mu) = \widehat{\varrho}_j\varpi_j(\mu) - \widehat{\varrho_j B_{rj}}G_{rj}\big(\dot{\Pi}_{dj}\big) - \widehat{\varrho_j B_{lj}}G_{lj}\big(\dot{\Pi}_{dj}\big). \tag{13}$$

Further, the compensation errors can be expressed as

$$\Pi_j(\mu) - \Pi_{dj}(\mu) = \widetilde{\varrho}_j\varpi_j(\mu) - \widetilde{\varrho_j B_{rj}}G_{rj}\big(\dot{\Pi}_{dj}\big) - \widetilde{\varrho_j B_{lj}}G_{lj}\big(\dot{\Pi}_{dj}\big) + g_{bj}(\mu). \tag{14}$$

Suppose that there exist positive constants $\bar{g}_j$ that satisfy $|g_{bj}(\mu)| \leq \bar{g}_j$ for any $\mu \geq 0$, $j = d, e, f$. Moreover, we define $\widehat{\vartheta}_j(\mu) = [\widehat{\varrho}_j, \widehat{\varrho_j B_{rj}}, \widehat{\varrho_j B_{lj}}]^T$, and $\nu_j = [\varpi_j, -G_{rj}(\dot{\Pi}_{dj}), -G_{lj}(\dot{\Pi}_{dj})]^T$, $j = d, e, f$. The compensation errors in (14) can be rewritten as

$$\Pi_j(\mu) - \Pi_{dj}(\mu) = \tilde{\vartheta}_j^T\nu_j + g_{bj}(\mu). \tag{15}$$

Assuming that the actuator input process does not work, the actual inputs $\Xi_j(\mu)$ are not equal to $\Pi_j(\mu)$, $j = d, e, f$. According to [30], the forms of the actual actuator inputs $\Xi_j(\mu)$ are defined as

$$\Xi_j(\mu) = \eta_j\Pi_j(\mu) + \Xi_{fj}(\mu) \tag{16}$$

where $\eta_j \in (0, 1]$, $j = d, e, f$, are unknown constants expressing the fault degree of the actuators and $\Xi_{fj}(\mu)$, $j = d, e, f$, represent the floating faults of the actuators, which are unknown functions. Thus, combining (15), the actual inputs can be expressed as

$$\Xi_j(\mu) = \eta_j\Pi_j(\mu) + \Xi_{fj}(\mu) = \eta_j\Pi_{dj}(\mu) + \eta_j\tilde{\vartheta}_j^T\nu_j + \eta_j g_{bj}(\mu) + \Xi_{fj}(\mu). \tag{17}$$

Remark 2: Equation (16) is a classic actuator error expression. If $\eta_j = 1$, they imply that the actuators are completely effective. Conversely, when $\eta_j = 0$, they denote that the actuators totally lose efficiency. In this article, we consider the incomplete loss of actuator efficiency, that is, $\eta_j \in (0, 1]$. $\Xi_{fj}(\mu)$ are time-varying parameters such that $\Xi_{fj}(\mu) \in [-\bar{\Xi}_{fj}, \bar{\Xi}_{fj}]$ with $\bar{\Xi}_{fj} > 0$.

Remark 3: In practical application, the BC of the riser system can be completed by a hydraulic system [31]. The hydraulic system converts the pressure energy of the liquid into mechanical energy through the hydraulic motor. However, incomplete contact between the two gears inside the hydraulic motor gearbox is inevitable, which is modeled as the backlash of the actuators (8). In addition, if the actuator structures are not continuously powered, actuator faults (16) will occur. It is worth noting that since there is only one actuator in each direction, the total loss of effectiveness fault or struck fault is not considered [32].

C. Fuzzy-Logic System Framework

Because of the excellent approximation performance of the FLS, it has been widely used in nonlinear system control in recent years [33]. Therefore, the FLS is used to compensate the unmodeled dynamics instead of the adaptive design of multiple parameters [29]. The FLS framework includes the fuzzifier, center-average defuzzifier, and product inference. The fuzzy rules are defined as follows [34]:

$$R^l : \text{IF } a_1 \text{ is } F_1^l, \ \ldots, \ a_n \text{ is } F_n^l$$
$$\text{THEN, } b \text{ is } Q^l, \ l = 1, 2, 3, \ldots, N$$

where $a = \{a_1, a_2, \ldots, a_n\}$ and b represent the fuzzy input and output, respectively; $\{F_1^l, \ldots, F_n^l, Q^l\} \in \mathcal{R}$ are fuzzy sets; and N denotes the number of fuzzy rules in the system. After fuzzification and defuzzification, we obtain the FLS output b as

$$b(a) = \frac{\sum_{l=1}^N \bar{b}_l \Big[\prod_{i=1}^n \zeta_{F_i^l}(a_i)\Big]}{\sum_{l=1}^N \Big[\prod_{i=1}^n \zeta_{F_i^l}(a_i)\Big]} \tag{18}$$

where $\zeta_{F_i^l}(a_i) = \exp[-(a_i - x_i^l)^2/y_i^l]$ denotes the system membership function, with x_i^l and y_i^l representing the centers and widths of $\zeta_{F_i^l}(x_i)$, respectively. In addition, $\bar{b}_l = \max_{b\in\mathcal{R}}\zeta_{Q^l}(a_i)$.

Then, we further express fuzzy output b as

$$b = \delta^T \epsilon(a) \tag{19}$$

where $\delta^T = [\bar{b}_1, \bar{b}_2, \ldots \bar{b}_N] = [\delta_1, \delta_2, \ldots, \delta_N]$ and $\epsilon(a) = [\epsilon_1(a), \epsilon_2(a), \ldots, \epsilon_N(a)]^T$. ϵ_l is given as

$$\epsilon_l = \frac{\prod_{i=1}^n \zeta_{F_i^l}(a_i)}{\sum_{l=1}^N \Big[\prod_{i=1}^n \zeta_{F_i^l}(a_i)\Big]}. \tag{20}$$

The target uncertainty compound items $\chi_j(a)$, $j = d, e, f$, are expressed as

$$\chi_j(a) = \Theta_{fj}(\mu) + \Gamma_j(\mu) = \delta_j^{\star T}\epsilon_j(a) + \beta_j(a). \tag{21}$$

According to [34], FLSs can approach a smooth continuous function defined on the set Ω_j to a certain extent. Then, we obtain

$$\sup_{a\in\Omega_j} \lim |\chi_j(a) - b_j(a)| \le \bar{\beta}_j \tag{22}$$

where $\bar{\beta}_j$, $j = d, e, f$, are positive constants.

D. Preliminaries

To facilitate the subsequent analysis, the following assumptions and lemmas are provided.

Assumption 1: For disturbances $\Gamma_j(\mu)$ and $\Phi_j(\omega, \mu)$, $j = d, e, f$, there exist positive constants $\bar{\Gamma}_j$ and $\bar{\Phi}_j$, $j = d, e, f$ satisfying $|\Gamma_d(\mu)| \le \bar{\Gamma}_d$, $|\Gamma_e(\mu)| \le \bar{\Gamma}_e$, $|\Gamma_f(\mu)| \le \bar{\Gamma}_f$, $|\Phi_d(\omega, \mu)| \le \bar{\Phi}_d$, $|\Phi_e(\omega, \mu)| \le \bar{\Phi}_e$, and $|\Phi_f(\omega, \mu)| \le \bar{\Phi}_f$.

Assumption 2: We assume that the unknown disturbances $\Gamma_j(\mu), j = d, e, f$, acting on the tip of the riser are related to vessel displacements $d(\tau, \mu)$, $e(\tau, \mu)$, and $f(\tau, \mu)$, and their respective derivatives $\dot{d}(\tau, \mu)$, $\dot{e}(\tau, \mu)$, and $\dot{f}(\tau, \mu)$, respectively.

Lemma 1 [35]: If p_j and r_j are scalars and satisfy $p_j \in \mathcal{R}, r_j \in \mathcal{R}^+$, $j = d, e, f$, we have

$$0 \le |p_j| - \frac{p_j^2}{\sqrt{p_j^2 + r_j^2}} \le r_j. \tag{23}$$

If $r_j > 0$ are uniformly bounded continuous functions with $\lim_{\mu\to\infty} \int_{\mu_0}^{\mu} r_j(\mu)d\mu \le \bar{r}_j$, the above inequalities are satisfied.

III. Control Design

In this section, the smoothing inverse operator for backlash compensation is introduced to obtain the compensation error and the designed input. Then, the external disturbances and model uncertainties are combined and approximated using the FLS. Subsequently, by combining the unknown backlash error with the time-varying actuator floating fault, an upper-bound adaptive compensation scheme is proposed.

A. Adaptive Fuzzy Fault-Tolerant Control

Let $q_j = (1/\eta_j)$, $j = d, e, f$. To achieve the control objectives, the following expected robust adaptive control commands are proposed:

$$\Pi_{dd} = -\hat{q}_d \Upsilon_{dd}, \ \Pi_{de} = -\hat{q}_e \Upsilon_{de}, \ \Pi_{df} = -\hat{q}_f \Upsilon_{df} \tag{24}$$

where $\hat{q}_j$, $j = d, e, f$, denote the estimated values of q_j with the estimated errors defined as $\tilde{q}_j = q_j - \hat{q}_j$. Υ_{dd}, Υ_{de}, and Υ_{df} are defined as

$$\Upsilon_{dd} = \frac{(d_{\tau\mu} + \pi\tau d_{\tau\omega})\hat{\sigma}_d^2}{\sqrt{(d_{\tau\mu} + \pi\tau d_{\tau\omega})^2\hat{\sigma}_d^2 + r_d^2(\mu)}} + \frac{\hat{\Lambda}_d(d_{\tau\mu} + \pi\tau d_{\tau\omega})}{4\iota_d\epsilon_1^T(a)\epsilon_1(a)} + m\pi\tau d_{\tau\omega\mu} + 2s_d d_{\tau\mu} \tag{25}$$

$$\Upsilon_{de} = \frac{(e_{\tau\mu} + \pi\tau e_{\tau\omega})\hat{\sigma}_e^2}{\sqrt{(e_{\tau\mu} + \pi\tau e_{\tau\omega})^2\hat{\sigma}_e^2 + r_e^2(\mu)}} + \frac{\hat{\Lambda}_e(e_{\tau\mu} + \pi\tau e_{\tau\omega})}{4\iota_e\epsilon_2^T(a)\epsilon_2(a)} + m\pi\tau e_{\tau\omega\mu} + 2s_e e_{\tau\mu} \tag{26}$$

$$\Upsilon_{df} = \frac{(f_{\tau\mu} + \pi\tau f_{\tau\omega})\hat{\sigma}_f^2}{\sqrt{(f_{\tau\mu} + \pi\tau f_{\tau\omega})^2\hat{\sigma}_f^2 + r_f^2(\mu)}} + \frac{\hat{\Lambda}_f(f_{\tau\mu} + \pi\tau f_{\tau\omega})}{4\iota_f\epsilon_3^T(a)\epsilon_3(a)} + m\pi\tau f_{\tau\omega\mu} + 2s_f f_{\tau\mu} \tag{27}$$

where $\pi, s_d, s_e, s_f, \iota_d, \iota_e, \iota_f > 0$, and $\hat{\Lambda}_j$, $j = d, e, f$, are the estimated values of $\Lambda_j^\star$ expressed as $\Lambda_j^\star = \|\delta_j^{\star T}\|^2$, with the estimation errors defined as $\tilde{\Lambda}_j = \Lambda_j^\star - \hat{\Lambda}_j$. Further, $\hat{\sigma}_j$, $j = d, e, f$, are the estimated values of σ_j defined as $\sigma_j = \sup\lim_{\mu\ge 0}|\eta_j g_{bj} + \Xi_{fj}|$, with the estimation errors represented as $\tilde{\sigma}_j = \sigma_j - \hat{\sigma}_j$. The terms $((j_{\tau\mu} + \pi\tau j_{\tau\omega})\hat{\sigma}_j^2/\sqrt{(j_{\tau\mu} + \pi\tau j_{\tau\omega})^2\hat{\sigma}_j^2 + r_j^2(\mu)})$, $j = d, e, f$, are used to compensate for the effects of the actuator float faults and inverse backlash dynamics compensation errors. $r_j(\mu)$, $j = d, e, f$, are three positive uniformly bounded integrable functions.

The dynamic adaptive update laws are designed as follows:

$$\dot{\hat{\Lambda}}_d = \frac{z_d(d_{\tau\mu} + \pi\tau d_{\tau\omega})^2}{4\iota_d\epsilon_1^T(a)\epsilon_1(a)} - \varepsilon_d\hat{\Lambda}_d \tag{28}$$

$$\dot{\hat{\Lambda}}_e = \frac{z_e\left(e_{\tau\mu} + \pi\tau e_{\tau\omega}\right)^2}{4\iota_e\epsilon_2^T(a)\epsilon_2(a)} - \varepsilon_e\hat{\Lambda}_e \tag{29}$$

$$\dot{\hat{\Lambda}}_f = \frac{z_f\left(f_{\tau\mu} + \pi\tau f_{\tau\omega}\right)^2}{4\iota_f\epsilon_3^T(a)\epsilon_3(a)} - \varepsilon_f\hat{\Lambda}_f \tag{30}$$

$$\dot{\hat{\vartheta}}_d = \mathrm{Proj}_{\vartheta_d}\left\{\Delta_d\left(d_{\tau\mu} + \pi\tau d_{\tau\omega}\right)\nu_d\right\} - \hat{\vartheta}_d \tag{31}$$

$$\dot{\hat{\vartheta}}_e = \mathrm{Proj}_{\vartheta_e}\left\{\Delta_e\left(e_{\tau\mu} + \pi\tau e_{\tau\omega}\right)\nu_e\right\} - \hat{\vartheta}_e \tag{32}$$

$$\dot{\hat{\vartheta}}_f = \mathrm{Proj}_{\vartheta_f}\left\{\Delta_f\left(f_{\tau\mu} + \pi\tau f_{\tau\omega}\right)\nu_f\right\} - \hat{\vartheta}_f \tag{33}$$

$$\dot{\hat{\sigma}}_d = \gamma_{\sigma d}\left(d_{\tau\mu} + \pi\tau d_{\tau\omega}\right) - \gamma_{\sigma d}\hat{\sigma}_d \tag{34}$$

$$\dot{\hat{\sigma}}_e = \gamma_{\sigma e}\left(e_{\tau\mu} + \pi\tau e_{\tau\omega}\right) - \gamma_{\sigma e}\hat{\sigma}_e \tag{35}$$

$$\dot{\hat{\sigma}}_f = \gamma_{\sigma f}\left(f_{\tau\mu} + \pi\tau f_{\tau\omega}\right) - \gamma_{\sigma f}\hat{\sigma}_f \tag{36}$$

$$\dot{\hat{q}}_d = \gamma_d\left(d_{\tau\mu} + \pi\tau d_{\tau\omega}\right)\Upsilon_{dd} - \hat{q}_d \tag{37}$$

$$\dot{\hat{q}}_e = \gamma_e\left(e_{\tau\mu} + \pi\tau e_{\tau\omega}\right)\Upsilon_{de} - \hat{q}_e \tag{38}$$

$$\dot{\hat{q}}_f = \gamma_f\left(f_{\tau\mu} + \pi\tau f_{\tau\omega}\right)\Upsilon_{df} - \hat{q}_f \tag{39}$$

where $\varepsilon_j, z_j, \gamma_{\eta j}, \gamma_j > 0, j = d, e, f$, and Δ_d, Δ_e, and $\Delta_f \in \mathcal{R}^{3\times 3}$, $j = d, e, f$, are all positive-definite symmetric matrices.

Remark 4: The reason for using $\mathrm{Proj}_{\vartheta_j}(\diamond)$ is to ensure that the estimated ϑ_j values are restricted within certain ranges. Clearly, if $\hat{\varrho}_j, j = d, e, f$, do not fall within the ranges, they can easily lead to a singularity when $\hat{\varrho}_j \to 0$, making the control inputs infinite. $\mathrm{Proj}_{\xi_j}(\diamond)$, $j = d, e, f$, describe the projection mappings defined in [36] as

$$\mathrm{Proj}_{\xi_j}(\diamond) = \begin{cases} \left(I - \Psi_j\frac{\nabla_{\xi_j}\nabla_{\xi_j}^T}{\nabla_{\xi_j}^T\Psi_j\nabla_{\xi_j}}\right)\diamond, \text{ if } \hat{\xi}_j \in \bar{\Omega}_j \\ \qquad\qquad \text{and } \nabla_{\xi_j}^T\diamond > 0, \\ (\diamond), \qquad \text{if } \hat{\xi}_j \in \hat{\Omega}_j \text{ or } \left(\hat{\xi}_j \in \bar{\Omega}_j\right. \\ \qquad\qquad \left.\text{and } \nabla_{\xi_j}^T\diamond \le 0\right) \end{cases} \tag{40}$$

where $\Psi_j \in \mathcal{R}^{3\times 3}$ are symmetric positive-definite matrices, $j = d, e, f$. $\hat{\Omega}_j$ and $\bar{\Omega}_j$, $j = d, e, f$, represent the interior of the sets Ω_j and the boundary of sets Ω_j, respectively. Further, ∇_{ξ_j}, $j = d, e, f$, denote the normal vectors that point outward when ξ_j, $j = d, e, f$, are at boundary $\bar{\Omega}_j$, and ξ_j represent the symbols replaced by ϑ_j in this article, $j = d, e, f$.

Remark 5: In the execution process, we can obtain signals $d_\tau, e_\tau, f_\tau, d_{\tau\mu}, e_{\tau\mu}, f_{\tau\mu}, d_{\tau\omega}, e_{\tau\omega}, f_{\tau\omega}, d_{\tau\omega\mu}, e_{\tau\omega\mu}$, and $f_{\tau\omega\mu}$ in control laws (24)–(27) through sensors and corresponding algorithms. Signals d_τ, e_τ, and f_τ can be measured by the laser displacement sensors and signals $d_{\tau\omega}, e_{\tau\omega}$, and $f_{\tau\omega}$ can be measured by inclinometers. In addition, the remaining signals $d_{\tau\mu}, e_{\tau\mu}, f_{\tau\mu}, d_{\tau\omega\mu}, e_{\tau\omega\mu}$, and $f_{\tau\omega\mu}$ can be further obtained by the backward difference algorithm based on the measured values. Furthermore, hydraulic motors are generally used to generate a control torque in practical industrial applications.

B. Stability Proof

We select a Lyapunov function $\digamma_k(\mu)$ as follows:

$$\digamma_k(\mu) = \digamma_{k1}(\mu) + \digamma_{k2}(\mu) + \digamma_{k3}(\mu) + \digamma_{k4}(\mu) \tag{41}$$

where

$$\begin{aligned} \digamma_{k1}(\mu) &= \frac{1}{2}EA\int_0^\tau\left[f_\omega + \frac{\left(d_\omega^2 + e_\omega^2\right)}{2}\right]^2 d\omega \\ &+ \frac{1}{2}EI\int_0^\tau\left(d_{\omega\omega}^2 + e_{\omega\omega}^2\right)d\omega + \frac{1}{2}T\int_0^\tau\left(d_\omega^2 + e_\omega^2\right)d\omega \\ &+ \frac{1}{2}\varsigma\int_0^\tau\left(d_\mu^2 + e_\mu^2 + f_\mu^2\right)d\omega \end{aligned} \tag{42}$$

$$\digamma_{k2}(\mu) = \pi\varsigma\int_0^\tau \omega\left(d_\mu d_\omega + e_\mu e_\omega + f_\mu f_\omega\right)d\omega \tag{43}$$

$$\begin{aligned} \digamma_{k3}(\mu) &= \frac{1}{2}m\left(d_{\tau\mu} + \pi\tau d_{\tau\omega}\right)^2 + \frac{1}{2}m\left(e_{\tau\mu} + \pi\tau e_{\tau\omega}\right)^2 \\ &+ \frac{1}{2}m\left(f_{\tau\mu} + \pi\tau f_{\tau\omega}\right)^2 \end{aligned} \tag{44}$$

$$\begin{aligned} \digamma_{k4}(\mu) &= \frac{1}{2z_d}\tilde{\Lambda}_d^2 + \frac{1}{2z_e}\tilde{\Lambda}_e^2 + \frac{1}{2z_f}\tilde{\Lambda}_f^2 + \frac{\eta_d}{2}\tilde{\vartheta}_d^T\Delta_d^{-1}\tilde{\vartheta}_d \\ &+ \frac{\eta_e}{2}\tilde{\vartheta}_e^T\Delta_e^{-1}\tilde{\vartheta}_e + \frac{\eta_f}{2}\tilde{\vartheta}_f^T\Delta_f^{-1}\tilde{\vartheta}_f + \frac{1}{2\gamma_{\sigma f}}\tilde{\sigma}_f^2 + \frac{\eta_d}{2\gamma_d}\tilde{q}_d^2 \\ &+ \frac{\eta_e}{2\gamma_e}\tilde{q}_e^2 + \frac{\eta_f}{2\gamma_f}\tilde{q}_f^2 + \frac{1}{2\gamma_{\sigma d}}\tilde{\sigma}_d^2 + \frac{1}{2\gamma_{\sigma e}}\tilde{\sigma}_e^2. \end{aligned} \tag{45}$$

Lemma 2 [37]: The Lyapunov candidate function given by (41) has upper and lower bounds

$$\begin{aligned} 0 &\le \varkappa_1[A(\mu) + \digamma_{k3}(\mu) + \digamma_{k4}(\mu)] \le \digamma_k(\mu) \\ &\le \varkappa_2[A(\mu) + \digamma_{k3}(\mu) + \digamma_{k4}(\mu)] \end{aligned} \tag{46}$$

where $\varkappa_1$ and $\varkappa_2$ are two positive constants and $A(\mu)$ is described as

$$\begin{aligned} A(\mu) \le \int_0^\tau &\left[d_\mu^2 + e_\mu^2 + f_\mu^2 + d_\omega^2 + e_\omega^2 + f_\omega^2\right. \\ &\left. + d_\omega^4 + e_\omega^4 + (d_\omega e_\omega)^2 + d_{\omega\omega}^2 + e_{\omega\omega}^2\right]d\omega. \end{aligned} \tag{47}$$

Proof: The proof process is similar to [25, Lemma 4]. ■

Lemma 3 [37]: The time derivative of (41) is upper bounded as

$$\dot{\digamma}_k(\mu) \le -\varkappa\digamma_k(\mu) + \theta \tag{48}$$

where $\varkappa$ and θ are two positive constants.

Proof: See the Appendix. ■

Theorem 1: For the riser-vessel system depicted in (1)–(7), with the established adaptive fuzzy FTC strategy (24) and online updating laws (28)–(39), if the initial conditions are bounded and the designed parameters are properly selected satisfying constraints (66)–(73), we conclude that the offsets of the riser system uniformly and ultimately converge to a small neighborhood around zero.

Proof: Using Lemma 3, we multiply (75) by $e^{\varkappa\mu}$ and integrate the resulting expression to obtain

$$\digamma_k(\mu) \le \digamma_k(0)e^{-\varkappa\mu} + \tfrac{\theta}{\varkappa}\left(1 - e^{-\varkappa\mu}\right). \tag{49}$$

Using $\digamma_{k1}(\mu)$, $A(\mu)$, and Lemma 2 yields

$$\frac{1}{\tau}d^2(\omega,\mu) \le \int_0^\tau d_\omega^2(\omega,\mu)d\omega \le A(\mu) \le \frac{1}{\varkappa_1}\digamma_k(\mu) \tag{50}$$

$$\frac{1}{\tau}e^2(\omega,\mu) \le \int_0^\tau e_\omega^2(\omega,\mu)d\omega \le A(\mu) \le \frac{1}{\varkappa_1}\digamma_k(\mu) \tag{51}$$

$$\frac{1}{\tau}f^2(\omega,\mu) \le \int_0^\tau f_\omega^2(\omega,\mu)d\omega \le A(\mu) \le \frac{1}{\varkappa_1}\digamma_k(\mu) \quad (52)$$

where $(\omega, \mu) \in [0, \tau] \times [0, +\infty)$. Substituting (50)–(52) into (49) yields

$$\lim_{\mu\to+\infty} |d(\omega,\mu)| \le \rho, \quad \lim_{\mu\to+\infty} |e(\omega,\mu)| \le \rho \quad (53)$$

$$\lim_{\mu\to+\infty} |f(\omega,\mu)| \le \rho \quad (54)$$

where $\omega \in [0, \tau]$ and $\rho = \sqrt{(\tau\theta/\varkappa_1\varkappa)}$. ■

IV. Numerical Simulation

To verify the effectiveness of the proposed FTC strategy, a numerical simulation is carried out using the finite difference method. The system parameters are presented as follows: $\tau = 1000$ m, $EI = 1.22 \times 10^5$ Nm^2, $m = 9.6 \times 10^6$ kg, $T = 2.75 \times 10^8$ N, $EA = 3.92 \times 10^8$ Nm^2, and $\varsigma = 108$ kg/m. In this study, the simulation time step and spatial displacement are set to $\Delta\mu = 0.06$ s and $\Delta\omega = 50$ m, respectively. The distributed disturbance of the system is detailed in [38]. According to Assumption 2, the distributed disturbances of the system are given as $\Gamma_d(\mu) = (d_\tau + d_{\tau\mu} + \sin(0.5t)) \times 10^4$, $\Gamma_e(\mu) = (e_\tau + e_{\tau\mu} + \sin(0.5t)) \times 10^4$, and $\Gamma_f(\mu) = (f_\tau + f_{\tau\mu} + \sin(0.5t)) \times 10^3$. The model uncertainties are considered as $\Theta_{fd} = 0.1(Td_{\tau\omega} + EAd_{\tau\omega}f_{\tau\omega} + EAd_{\tau\omega}e_{\tau\omega}^2 - EId_{\tau\omega\omega\omega})$, $\Theta_{fe} = 0.1(Te_{\tau\omega} + EAe_{\tau\omega}f_{\tau\omega} + EAe_{\tau\omega}d_{\tau\omega}^2 - EIe_{\tau\omega\omega\omega})$, and $\Theta_{ff} = 0.1(EAf_{\tau\omega} + EAd_{\tau\omega}^2 + EAe_{\tau\omega}^2)$. The initial states of the system are $d(\omega, 0) = e(\omega, 0) = f(\omega, 0) = (4\omega/\tau)$ and $d_\mu(\omega, 0) = e_\mu(\omega, 0) = f_\mu(\omega, 0) = 0$. The parameter settings of the proposed controllers are presented as follows $s_d = s_e = 1.6 \times 10^7$, $s_f = 1 \times 10^6$, $z_d = z_e = 0.04$, $z_f = 0.05$, $\varepsilon_d = \varepsilon_e = \varepsilon_f = 1 \times 10^{-3}$, $\pi = 4.9 \times 10^{-4}$, $\Delta_d = \Delta_e = \Delta_f = 10^{-3}\Gamma^{3\times3}$, $\gamma_d = \gamma_e = 1.28 \times 10^{-4}$, $\gamma_f = 1.2 \times 10^{-3}$, $\gamma_{\sigma d} = \gamma_{\sigma e} = \gamma_{\sigma f} = 1$, $\iota_d = \iota_e = 50$, $\iota_f = 100$, and $P_d = P_e = P_f = 20$. In this study, the FLS inputs $\{a_1, a_2, \ldots, a_n\}$ are set to $\{d_{\tau\omega}, e_{\tau\omega}, f_{\tau\omega}, d_{\tau\mu}, d_{\tau\omega\mu}\}$, $\{d_{\tau\omega}, e_{\tau\omega}, f_{\tau\omega}, e_{\tau\mu}, e_{\tau\omega\mu}\}$, and $\{d_{\tau\omega}, e_{\tau\omega}, f_{\tau\omega}, f_{\tau\mu}, f_{\tau\omega\mu}\}$. We choose the fuzzy membership functions for the system states $a_1, a_2, \ldots a_n$ as follows:

$$\zeta_{F_i^l}(a_i) = \exp\left[-(a_i + 1 - (l-1))^2\right] \quad (55)$$

where $l = 1, \ldots, 5$. The fuzzy basis functions are defined as

$$\epsilon_i(a) = \frac{\prod_{i=1}^5 \zeta_{F_i^l}(a_i)}{\sum_{l=1}^5\left[\prod_{i=1}^5 \zeta_{F_i^l}(a_i)\right]}. \quad (56)$$

For the loss of the actuator effectiveness fault, the efficiency factors are set to $\eta_d = \eta_e = \eta_f = 0.5$ and $\Xi_{fd}(\mu) = \Xi_{fe}(\mu) = \Xi_{ff}(\mu) = 100\sin\mu$. In addition, the actuator clearance parameters are chosen as $\vartheta_d = \vartheta_e = \vartheta_f = [1, 3 \times 10^5, -2 \times 10^5]$. The limit values are given as $\vartheta_{d\min} = \vartheta_{e\min} = \vartheta_{f\min} = [0.8, 2.16 \times 10^5, -2.4 \times 10^5]$, and $\vartheta_{d\max} = \vartheta_{e\max} = \vartheta_{f\max} = [1.2, 3.96 \times 10^5, -1.92 \times 10^5]$.

When no control was applied ($\Xi_d = \Xi_e = \Xi_f = 0$), as shown in Fig. 2, the system freely vibrated in a 3-D space. The maximum deflection can reach 4 m, which has significant side effects for pipeline transportation. Under the adaptive fuzzy FTC depicted in (24)–(39), we can observe a control effect

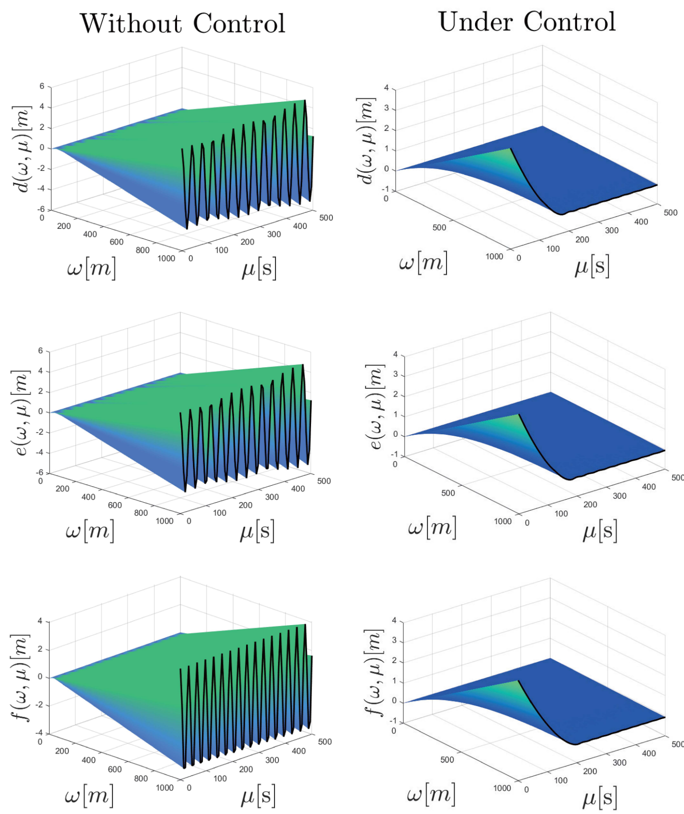

Fig. 2. 3-D offset of the riser.

from Fig. 2. It can be seen that the 3-D direction deflection of the riser system can be stabilized under control.

Fig. 3 shows the time variation diagrams of the actual inputs Ξ_d, Ξ_e, and Ξ_f and expected inputs ϖ_d, ϖ_e, and ϖ_f, respectively. Therefore, with the designed controller, the actual outputs are affected by the faults; however, effective controls can still be achieved. Compared with previous studies [13], [15], [16], the actual inputs do not produce chattering under the influence of backlash, which proves the effectiveness of the smooth inverse backlash dynamics (12).

V. Conclusion

In this article, a new adaptive fuzzy FTC strategy was proposed to stabilize a 3-D riser-vessel system affected by actuator faults, unknown backlash nonlinearity, and model uncertainty. Smooth inverse backlash dynamics were utilized to address the chattering caused by the previous unsmooth inverse operator. The FLS was introduced to compensate for the influence of unknown disturbances and model uncertainties. Further, an unknown upper-bound adaptive compensation strategy was proposed to offset the side effects caused by the inverse operator compensation error and actuator floating fault. The designed control guaranteed uniform boundedness of the controlled system. The control performance was further evaluated by applying theoretical and simulation analyses. Despite its many advantages, the proposed control strategy cannot be applied to actuator stuck-type faults [39], [40] or intermittent actuator faults [41]. When the system actuator is stuck or the efficiency factor changes, the controlled system may no longer be stable. This problem will be addressed in future

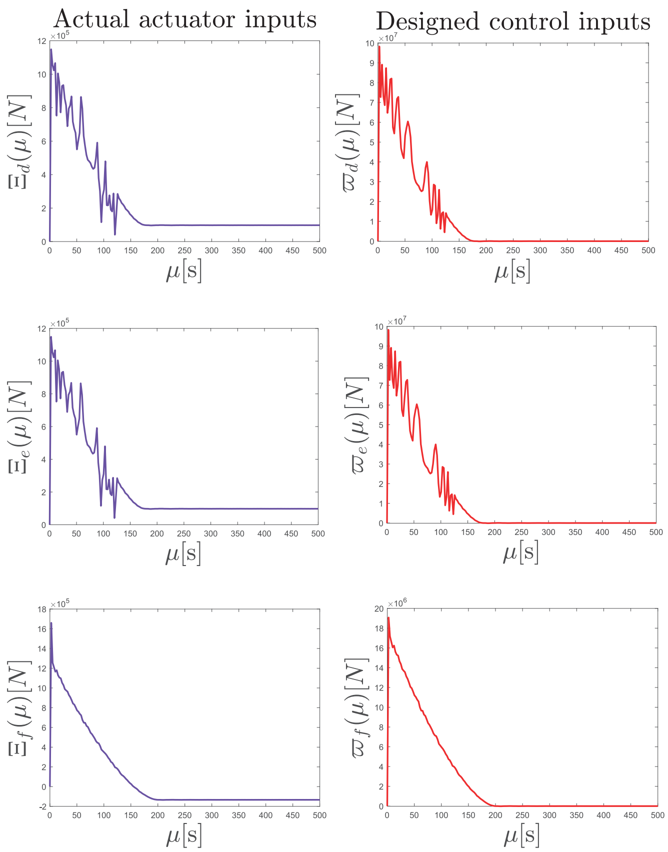

Fig. 3. 3-D control inputs of the riser.

work. Moreover, the iterative learning control of controlled riser-vessel systems will also be addressed in future work.

Appendix

Proof of Lemma 3

Proof: We differentiate (41) to derive the following:

$$\dot{F}_k(\mu) = \dot{F}_{k1}(\mu) + \dot{F}_{k2}(\mu) + \dot{F}_{k3}(\mu) + \dot{F}_{k4}(\mu). \quad (57)$$

Function $\dot{F}_{k1}(\mu)$ yields

$$\begin{aligned}\dot{F}_{k1}(\mu) = &\left(\Xi_d + \Gamma_d + \Theta_{fd} - md_{\tau\mu\mu}\right)d_{\tau\mu} + (\Xi_e + \Gamma_e \\ &+\Theta_{fe} - me_{\tau\mu\mu})e_{\tau\mu} + \left(\Xi_f + \Gamma_f + \Theta_{ff} \right.\\ &\left.-mf_{\tau\mu\mu}\right)f_{\tau\mu} + \int_0^\tau \left[d_\mu\Phi_d + e_\mu\Phi_e + f_\mu\Phi_f\right]d\omega. \quad (58)\end{aligned}$$

Moreover, the derivative of Lyapunov function $\dot{F}_{k2}(\mu)$ is given as

$$\begin{aligned}\dot{F}_{k2}(\mu) = &-\frac{3}{8}\pi EA\int_0^\tau d_\omega^4 d\omega - \frac{3}{8}\pi EA\int_0^\tau e_\omega^4 d\omega \\ &-\pi EA\int_0^\tau f_\omega d_\omega^2 d\omega - \pi EA\int_0^\tau f_\omega e_\omega^2 d\omega \\ &-\frac{3}{4}\pi EA\int_0^\tau (d_\omega e_\omega)^2 d\omega - \frac{3}{2}\pi EI\int_0^\tau d_{\omega\omega}^2 d\omega \\ &-\frac{3}{2}\pi EI\int_0^\tau e_{\omega\omega}^2 d\omega - \frac{1}{2}\pi T\int_0^\tau d_\omega^2 d\omega \\ &-\frac{1}{2}\pi T\int_0^\tau e_\omega^2 d\omega - \frac{1}{2}\pi EA\tau\left[\frac{1}{2}d_{\tau\omega}^2\right. \\ &\left.+\frac{1}{2}e_{\tau\omega}^2 + f_{\tau\omega}\right]^2 - \frac{1}{2}\pi T\tau d_{\tau\omega}^2 \\ &-\frac{1}{2}\pi EA\int_0^\tau f_\omega^2 d\omega - \frac{1}{2}\pi\varsigma\int_0^\tau d_\mu^2 d\omega \\ &-\frac{1}{2}\pi\varsigma\int_0^\tau e_\mu^2 d\omega - \frac{1}{2}\pi\varsigma\int_0^\tau f_\mu^2 d\omega \\ &+\pi\tau f_{\tau\omega}\left(\Xi_f + \Gamma_f + \Theta_{ff} - mf_{\tau\mu\mu}\right) \\ &+\frac{1}{2}\pi\varsigma\tau\left[d_{\tau\mu}^2 + e_{\tau\mu}^2 + f_{\tau\mu}^2\right] \\ &-\frac{1}{2}\pi T\tau e_{\tau\omega}^2 + \pi\tau d_{\tau\omega}\left(\Xi_d + \Gamma_d + \Theta_{fd}\right. \\ &\left.-md_{\tau\mu\mu}\right) + \pi\tau e_{\tau\omega}\left(\Xi_e + \Gamma_e + \Theta_{fe} - me_{\tau\mu\mu}\right) \\ &+\pi\int_0^\tau \omega\left(d_\omega\Phi_d + e_\omega\Phi_e + f_\omega\Phi_f\right)d\omega. \quad (59)\end{aligned}$$

Subsequently, we take the derivative of $F_{k3}(\mu)$

$$\begin{aligned}\dot{F}_{k3}(\mu) = &\left(d_{\tau\mu} + \pi\tau d_{\tau\omega}\right)\left(md_{\tau\mu\mu} + m\pi\tau d_{\tau\omega\mu}\right) \\ &+\left(e_{\tau\mu} + \pi\tau e_{\tau\omega}\right)\left(me_{\tau\mu\mu} + m\pi\tau e_{\tau\omega\mu}\right) \\ &+\left(f_{\tau\mu} + \pi\tau f_{\tau\omega}\right)\left(mf_{\tau\mu\mu} + m\pi\tau f_{\tau\omega\mu}\right). \quad (60)\end{aligned}$$

The derivation of function $F_{k4}(\mu)$ yields

$$\begin{aligned}\dot{F}_{k4}(\mu) = &-\frac{\tilde{\Lambda}_d\left(d_{\tau\mu} + \pi\tau d_{\tau\omega}\right)^2}{4\iota_d\epsilon_1^T(a)\epsilon_1(a)} + \eta_d\tilde{\vartheta}_d^T\Delta_d^{-1}\hat{\vartheta}_d \\ &-\frac{\tilde{\Lambda}_e\left(e_{\tau\mu} + \pi\tau e_{\tau\omega}\right)^2}{4\iota_e\epsilon_2^T(a)\epsilon_2(a)} + \frac{\eta_d}{\gamma_d}\tilde{q}_d\hat{q}_d + \frac{\varepsilon_d}{z_d}\tilde{\Lambda}_d\hat{\Lambda}_d \\ &+\frac{\varepsilon_e}{z_e}\tilde{\Lambda}_e\hat{\Lambda}_e - \frac{\tilde{\Lambda}_f\left(f_{\tau\mu} + \pi\tau f_{\tau\omega}\right)^2}{4\iota_f\epsilon_3^T(a)\epsilon_3(a)} + \frac{\varepsilon_f}{z_f}\tilde{\Lambda}_f\hat{\Lambda}_f \\ &-\eta_d\tilde{\vartheta}_d^T\Delta_d^{-1}\mathrm{Proj}\left[\Delta_d\left(d_{\tau\mu} + \pi\tau d_{\tau\omega}\right)\nu_d\right] \\ &-\eta_e\tilde{\vartheta}_e^T\Delta_e^{-1}\mathrm{Proj}\left[\Delta_e\left(e_{\tau\mu} + \pi\tau e_{\tau\omega}\right)\nu_e\right] \\ &-\eta_f\tilde{\vartheta}_f^T\Delta_f^{-1}\mathrm{Proj}\left[\Delta_f\left(f_{\tau\mu} + \pi\tau f_{\tau\omega}\right)\nu_f\right] \\ &-\eta_d\tilde{q}_d\left(d_{\tau\mu} + \pi\tau d_{\tau\omega}\right)\Upsilon_{dd} - \tilde{\sigma}_d\left(d_{\tau\mu} + \pi\tau d_{\tau\omega}\right) \\ &-\eta_e\tilde{q}_e\left(e_{\tau\mu} + \pi\tau e_{\tau\omega}\right)\Upsilon_{de} + \frac{\eta_e}{\gamma_e}\tilde{q}_e\hat{q}_e + \hat{\sigma}_d\tilde{\sigma}_d \\ &-\eta_f\tilde{q}_f\left(f_{\tau\mu} + \pi\tau f_{\tau\omega}\right)\Upsilon_{df} + \frac{\eta_f}{\gamma_f}\tilde{q}_f\hat{q}_f + \hat{\sigma}_e\tilde{\sigma}_e \\ &-\tilde{\sigma}_e\left(e_{\tau\mu} + \pi\tau e_{\tau\omega}\right) - \tilde{\sigma}_f\left(f_{\tau\mu} + \pi\tau f_{\tau\omega}\right) \\ &+\eta_f\tilde{\vartheta}_f^T\Delta_f^{-1}\hat{\vartheta}_f + \hat{\sigma}_f\tilde{\sigma}_f + \eta_e\tilde{\vartheta}_e^T\Delta_e^{-1}\hat{\vartheta}_e. \quad (61)\end{aligned}$$

According to $0 < \epsilon_i^T(a)\epsilon_i(a) \leq 1$, $i = 1, 2, 3$, the following inequalities can be obtained after further derivation:

$$\begin{aligned}&\left(d_{\tau\mu} + \pi\tau d_{\tau\omega}\right)\delta_d^{\star T}\epsilon_1(a) \leq \frac{\left(d_{\tau\mu} + \pi\tau d_{\tau\omega}\right)^2\left[\delta_d^{\star T}\epsilon_1(a)\right]^2}{4\iota_d} \\ &+\iota_d \leq \frac{\left(d_{\tau\mu} + \pi\tau d_{\tau\omega}\right)^2\Lambda_d^\star\epsilon_1^T(a)\epsilon_1(a)}{4\iota_d} + \iota_d \\ &\leq \iota_d + \frac{\left(d_{\tau\mu} + \pi\tau d_{\tau\omega}\right)^2\Lambda_d^\star}{4\iota_d\epsilon_1^T(a)\epsilon_1(a)} \quad (62)\end{aligned}$$

$$\left(d_{\tau\mu} + \pi\tau d_{\tau\omega}\right)\beta_d(a) \leq \frac{1}{4}\left(d_{\tau\mu} + \pi\tau d_{\tau\omega}\right)^2 + \beta_d^{\star 2} \quad (63)$$

$$\tilde{\sigma}_d\hat{\sigma}_d = \tilde{\sigma}_d(\sigma_d - \tilde{\sigma}_d) \leq \left(-\tilde{\sigma}_d^2 + \frac{1}{2}\tilde{\sigma}_d^2 + \frac{1}{2}\sigma_d^2\right) = \frac{1}{2}\sigma_d^2 - \frac{1}{2}\tilde{\sigma}_d^2 \tag{64}$$

where $|\beta_d| \leq \beta_d^\star$ with $\beta_d^\star$ is a positive constant. The derivation of polarization terms e_τ and f_τ is similar to that of d_τ and will not be expanded upon here.

Invoking (41), (62)–(64), $(1/2)d_{\tau\omega}^2 \geq f_{\tau\omega}^2$, $(1/2)e_{\tau\omega}^2 \geq f_{\tau\omega}^2$, and $\tilde{\xi}_j^T\Gamma_j^{-1}(\diamond - \mathrm{Proj}_{\xi_j}(\diamond)) \leq 0, j = d, e, f$. Applying Lemmas 1, Young's inequality [25, Lemma 1], Sobolev's inequality [25, Lemma 2], and Assumptions 1 and 2, the proposed adaptive laws (28)–(39) and control laws (24)–(27) are substituted into the differentiation of $\digamma_k(\mu)$

$$\begin{aligned}
\dot{\digamma}_k(\mu) \leq & -\left(\frac{1}{2}\pi\varsigma - \frac{1}{\alpha_1}\right)\int_0^\tau d_\mu^2 d\omega - \left(s_d - \frac{1}{2}\pi\varsigma\tau\right)d_{\tau\mu}^2 \\
& -\left(\frac{1}{2}\pi\varsigma - \frac{1}{\alpha_2}\right)\int_0^\tau e_\mu^2 d\omega - \left(s_e - \frac{1}{2}\pi\varsigma\tau\right)e_{\tau\mu}^2 \\
& -\left(\frac{1}{2}\pi\varsigma - \frac{1}{\alpha_3}\right)\int_0^\tau f_\mu^2 d\omega - \left(s_f - \frac{1}{2}\pi\varsigma\tau\right)f_{\tau\mu}^2 \\
& -\left(\frac{1}{2}\pi EA - \pi\tau\alpha_6\right)\int_0^\tau f_\omega^2 d\omega - \left(\frac{3}{8}\pi EA\right. \\
& \left.-\frac{\pi EA}{2\alpha_7}\right)\int_0^\tau d_\omega^4 d\omega - \frac{\varepsilon_d}{2z_d}\tilde{\Lambda}_d^2 + \frac{\varepsilon_e}{2z_e}\Lambda_e^{\star 2} \\
& -\left(\frac{3}{8}\pi EA - \frac{\pi EA}{2\alpha_8}\right)\int_0^\tau e_\omega^4 d\omega + \beta_d^{\star 2} \\
& -\left(\frac{1}{2}\pi T - \pi\tau\alpha_4 - \frac{\pi EA\alpha_7}{4}\right)\int_0^\tau d_\omega^2 d\omega \\
& -\left(\frac{1}{2}\pi T - \pi\tau\alpha_5 - \frac{\pi EA\alpha_8}{4}\right)\int_0^\tau e_\omega^2 d\omega \\
& +\left(\alpha_1 + \frac{\pi\tau}{\alpha_4}\right)\int_0^\tau \Phi_d^2 d\omega + \left(\alpha_2 + \frac{\pi\tau}{\alpha_5}\right)\int_0^\tau \Phi_e^2 d\omega \\
& +\left(\alpha_3 + \frac{\pi\tau}{\alpha_6}\right)\int_0^\tau \Phi_f^2 d\omega - \frac{3}{2}\pi EI\int_0^\tau d_{\omega\omega}^2 d\omega \\
& -\frac{3}{2}\pi EI\int_0^\tau e_{\omega\omega}^2 d\omega - \frac{3}{4}\pi EA\int_0^\tau (d_\omega e_\omega)^2 d\omega \\
& -\left(\frac{1}{4}\pi T\tau - s_d\pi^2\tau^2\right)d_{\tau\omega}^2 - \frac{\varepsilon_f}{2z_f}\tilde{\Lambda}_f^2 - \frac{\eta_d}{2\gamma_d}\tilde{q}_d^2 \\
& -\left(\frac{1}{4}\pi T\tau - s_e\pi^2\tau^2\right)e_{\tau\omega}^2 - \frac{\varepsilon_e}{2z_e}\tilde{\Lambda}_e^2 + \frac{\varepsilon_f}{2z_f}\Lambda_f^{\star 2} \\
& -\left(\pi T\tau - s_f\pi^2\tau^2\right)f_{\tau\omega}^2 + \beta_e^{\star 2} + \beta_f^{\star 2} + \frac{\varepsilon_d}{2z_d}\Lambda_d^{\star 2} \\
& -\left(s_f - \frac{1}{4}\right)(f_{\tau\mu} + \pi\tau f_{\tau\omega})^2 + \frac{\eta_d}{2\gamma_d}q_d^2 - \frac{\eta_e}{2\gamma_e}\tilde{q}_e^2 \\
& -\left(s_d - \frac{1}{4}\right)(d_{\tau\mu} + \pi\tau d_{\tau\omega})^2 + \frac{\eta_e}{2\gamma_e}q_e^2 - \frac{\eta_f}{2\gamma_f}\tilde{q}_f^2 \\
& -\left(s_e - \frac{1}{4}\right)(e_{\tau\mu} + \pi\tau e_{\tau\omega})^2 - \frac{\eta_f}{2}\frac{\tilde{\vartheta}_f^T\Delta_f^{-1}\tilde{\vartheta}_f}{\lambda_{\mathrm{fmax}}\left(\Delta_f^{-1}\right)} \\
& +r_e(\mu) + \frac{1}{2}\sigma_e^2 - \frac{1}{2}\tilde{\sigma}_e^2 - \frac{\eta_d}{2}\frac{\tilde{\vartheta}_d^T\Delta_d^{-1}\tilde{\vartheta}_d}{\lambda_{\mathrm{dmax}}\left(\Delta_d^{-1}\right)} \\
& -\frac{1}{2}\pi EA\tau\left[\frac{1}{2}d_{\tau\omega}^2 + \frac{1}{2}e_{\tau\omega}^2 + f_{\tau\omega}\right]^2 + \frac{1}{2}\vartheta_{fm}^2 \\
& +\frac{\eta_f}{2\gamma_f}q_f^2 + r_d(\mu) + \frac{1}{2}\sigma_d^2 - \frac{1}{2}\tilde{\sigma}_d^2 + \frac{1}{2}\vartheta_{dm}^2 \\
& +r_f(\mu) + \frac{1}{2}\sigma_f^2 - \frac{1}{2}\tilde{\sigma}_f^2 - \frac{\eta_e}{2}\frac{\tilde{\vartheta}_e^T\Delta_e^{-1}\tilde{\vartheta}_e}{\lambda_{\mathrm{emax}}\left(\Delta_e^{-1}\right)} \\
& +\frac{1}{2}\vartheta_{em}^2 + \iota_d + \iota_e + \iota_f
\end{aligned} \tag{65}$$

where $|\beta_e| \leq \beta_e^\star$ and $|\beta_f| \leq \beta_f^\star$ with $\beta_e^\star$ and $\beta_f^\star$ are two positive constants. In addition, $\alpha_1 \sim \alpha_8 > 0$ and parameters π, s_d, s_e, s_f, α_i, and $i = 1\cdots 8$ are chosen to satisfy the following constraints (66)–(73). Owing to the existence of adaptive mapping operators, three constants, ϑ_{dm}, ϑ_{em}, and $\vartheta_{fm} > 0$, are guaranteed to exist satisfying $\|\tilde{\vartheta}_d\| \leq \vartheta_{dm}$, $\|\tilde{\vartheta}_e\| \leq \vartheta_{em}$, and $\|\tilde{\vartheta}_f\| \leq \vartheta_{fm}$, respectively.

The constraint conditions making (65) hold are formulated as

$$\kappa_1 = \frac{1}{2}\pi\varsigma - \frac{1}{\alpha_1} > 0,\ \kappa_2 = \frac{1}{2}\pi\varsigma - \frac{1}{\alpha_2} > 0 \tag{66}$$

$$\kappa_3 = \frac{1}{2}\pi\varsigma - \frac{1}{\alpha_3} > 0,\ \kappa_4 = \frac{1}{2}T - \tau\alpha_4 - \frac{EA\alpha_7}{4} > 0 \tag{67}$$

$$\kappa_5 = s_d - \frac{1}{2}\pi\varsigma\tau > 0,\ \kappa_6 = \frac{1}{2}EA - \tau\alpha_6 > 0 \tag{68}$$

$$\kappa_7 = \frac{3}{8}EA - \frac{EA}{2\alpha_7} > 0,\ \kappa_8 = \frac{3}{8}EA - \frac{EA}{2\alpha_8} > 0 \tag{69}$$

$$\kappa_9 = s_f - \frac{1}{2}\pi\varsigma\tau > 0,\ \kappa_{10} = s_e - \frac{1}{2}\pi\varsigma\tau > 0 \tag{70}$$

$$\kappa_{11} = \frac{1}{2}T - \tau\alpha_5 - \frac{EA\alpha_8}{4} > 0,\ T \geq 4s_d\pi\tau \tag{71}$$

$$s_d > \frac{1}{4},\ s_e > \frac{1}{4},\ s_f > \frac{1}{4},\ T \geq 4s_e\pi\tau,\ T \geq s_f\pi\tau \tag{72}$$

$$\begin{aligned}
\theta = & \left(\alpha_1 + \frac{\pi\tau}{\alpha_4}\right)\tau\bar{\Phi}_d^2 + \left(\alpha_2 + \frac{\pi\tau}{\alpha_5}\right)\tau\bar{\Phi}_e^2 + \left(\alpha_3 + \frac{\pi\tau}{\alpha_6}\right)\tau\bar{\Phi}_f^2 \\
& +\frac{1}{2}\vartheta_{dm}^2 + \frac{1}{2}\vartheta_{em}^2 + \frac{1}{2}\vartheta_{fm}^2 + \bar{r}_d + \bar{r}_e + \bar{r}_f + h_d + h_e \\
& +\frac{\varepsilon_d}{2z_d}\Lambda_d^{\star 2} + \frac{\varepsilon_e}{2z_e}\Lambda_e^{\star 2} + \frac{\varepsilon_f}{2z_f}\Lambda_f^{\star 2} + \frac{\eta_d}{2\gamma_d}q_d^2 + h_f \\
& +\frac{\eta_e}{2\gamma_e}q_e^2 + \frac{\eta_f}{2\gamma_f}q_f^2 + \beta_d^{\star 2} + \beta_e^{\star 2} + \beta_f^{\star 2} < +\infty
\end{aligned} \tag{73}$$

where $h_j = (1/2)\sigma_j^2$, $j = d, e, f$.

Invoking (66)–(73), we obtain

$$\begin{aligned}
\dot{\digamma}_k(\mu) \leq & -\kappa_1\int_0^\tau d_\mu^2 d\omega - \kappa_2\int_0^\tau e_\mu^2 dz - \kappa_3\int_0^\tau f_\mu^2 d\omega \\
& -\kappa_4\pi\int_0^\tau d_\omega^2 d\omega - \kappa_5 d_{\tau\mu}^2 - \kappa_6\pi\int_0^\tau f_\omega^2 d\omega \\
& -\kappa_7\pi\int_0^\tau d_\omega^4 d\omega - \kappa_8\pi\int_0^\tau e_\omega^4 d\omega - \frac{\varepsilon_f}{2z_f}\tilde{\Lambda}_f^2 \\
& -\frac{3}{2}\pi EI\int_0^\tau d_{\omega\omega}^2 d\omega - \left(s_e - \frac{1}{4}\right)(e_{\tau\mu} + \pi\tau e_{\tau\omega})^2 \\
& -\kappa_9 e_{\tau\mu}^2 - \kappa_{10} f_{\tau\mu}^2 - \kappa_{11}\pi\int_0^\tau e_\omega^2 d\omega \\
& -\frac{3}{2}\pi EI\int_0^\tau e_{\omega\omega}^2 d\omega - \frac{\varepsilon_d}{2z_d}\tilde{\Lambda}_d^2 - \frac{\varepsilon_e}{2z_e}\tilde{\Lambda}_e^2 \\
& -\frac{3}{4}\pi EA\int_0^\tau (d_\omega e_\omega)^2 d\omega - \frac{\eta_e}{2\gamma_e}\tilde{q}_e^2 - \frac{\eta_f}{2\gamma_f}\tilde{q}_f^2
\end{aligned}$$

$$
\begin{aligned}
&-\left(s_d-\frac{1}{4}\right)(d_{\tau\mu}+\pi\tau d_{\tau\omega})^2-\frac{\eta_d}{2}\frac{\tilde{\vartheta}_d^T\Delta_d^{-1}\tilde{\vartheta}_d}{\lambda_{\mathrm{dmax}}\left(\Delta_d^{-1}\right)}\\
&-\left(s_f-\frac{1}{4}\right)(f_{\tau\mu}+\pi\tau f_{\tau\omega})^2-\frac{\eta_d}{2\gamma_d}\tilde{q}_d^2\\
&-\frac{\eta_e}{2}\frac{\tilde{\vartheta}_e^T\Delta_b^{-1}\tilde{\vartheta}_e}{\lambda_{\mathrm{emax}}\left(\Delta_e^{-1}\right)}-\frac{\eta_f}{2}\frac{\tilde{\vartheta}_f^T\Delta_f^{-1}\tilde{\vartheta}_f}{\lambda_{\mathrm{fmax}}\left(\Delta_f^{-1}\right)}\\
&-\frac{1}{2}\tilde{\sigma}_d^2-\frac{1}{2}\tilde{\sigma}_e^2-\frac{1}{2}\tilde{\sigma}_f^2+\theta\\
\le\ &-\varkappa_3(A(\mu)+F_{k3}(\mu)+F_{k4}(\mu))+\theta
\end{aligned}
\tag{74}
$$

where $\varkappa_3 = \min(\kappa_1, \kappa_2, \kappa_3, \kappa_4\pi, \kappa_5, \kappa_6\pi, \kappa_7\pi, \kappa_8\pi, \kappa_9, \kappa_{10}, \kappa_{11}\pi, (3/2)\pi EI, (3/4)\pi EA, [(2s_d-0.5)/m], [(2s_e-0.5)/m], [(2s_f-0.5)/m], [1/\lambda_{\mathrm{dmax}}(\Delta_d^{-1})], [1/\lambda_{\mathrm{emax}}(\Delta_e^{-1})], [1/\lambda_{\mathrm{fmax}}(\Delta_f^{-1})], \varepsilon_d, \varepsilon_e, \varepsilon_f, \gamma_{\sigma d}, \gamma_{\sigma e}, \gamma_{\sigma f}, 1)$.

Invoking (74), we further obtain

$$\dot{F}_k(\mu) \le -\varkappa F_k(\mu) + \theta \tag{75}$$

where $\varkappa = (\varkappa_3/\varkappa_2)$. This completes the proof. ■

REFERENCES

[1] K. D. Do, "Inverse optimal gain assignment control of evolution systems and its application to boundary control of marine risers," *Automatica*, vol. 106, pp. 242–256, Aug. 2019.

[2] Y. Feng, Y. Wang, J.-W. Wang, and H.-X. Li, "Backstepping-based distributed abnormality localization for linear parabolic distributed parameter systems," *Automatica*, vol. 135, 2022, Art. no. 109930.

[3] B. Chentouf and S. Mansouri, "Stabilization of an overhead crane system with infinite memory in the boundary control," *IEEE Trans. Autom. Control*, early access, Sep. 13, 2022, doi: 10.1109/TAC.2022.3206250.

[4] Z. Zhao, Z. Tan, Z. Liu, M. O. Efe, and C. K. Ahn, "Adaptive inverse compensation fault-tolerant control for a flexible manipulator with unknown dead-zone and actuator faults," *IEEE Trans. Ind. Electron.*, vol. 70, no. 12, pp. 12698–12707, 2023.

[5] Y. Liu, Y. Wang, Y. Feng, and Y. Wu, "Neural network-based adaptive boundary control of a flexible riser with input deadzone and output constraint," *IEEE Trans. Cybern.*, vol. 52, no. 12, pp. 13120–13128, Dec. 2022.

[6] Y. Liu, Y. Wang, Y. Mei, and Y. Wu, "Boundary iterative learning control of a flexible riser with input saturation and output constraint," *IEEE Trans. Syst., Man, Cybern., Syst.*, vol. 52, no. 11, pp. 7044–7052, Nov. 2022.

[7] Z. Zhao, C. K. Ahn, and H.-X. Li, "Dead zone compensation and adaptive vibration control of uncertain spatial flexible riser systems," *IEEE/ASME Trans. Mechatronics*, vol. 25, no. 3, pp. 1398–1408, Jun. 2020.

[8] Z. Zhao, Y. Liu, T. Zou, and K.-S. Hong, "Robust adaptive control of a riser-vessel system in three-dimensional space," *IEEE Trans. Syst., Man, Cybern., Syst.*, vol. 52, no. 7, pp. 4447–4456, Jul. 2022.

[9] L. Sun, X. Li, L. Chen, H. Shi, and Z. Jiang, "Dual-motor coordination for high-quality servo with transmission backlash," *IEEE Trans. Ind. Electron.*, vol. 70, no. 2, pp. 1182–1196, Feb. 2023.

[10] Z. Lyu, Z. Liu, K. Xie, C. L. P. Chen, and Y. Zhang, "Adaptive tracking control for switched nonlinear systems with fuzzy actuator backlash," *Fuzzy Sets Syst.*, vol. 385, pp. 60–80, Apr. 2020.

[11] G. Tao and P. V. Kokotovic, "Continuous-time adaptive control of systems with unknown backlash," *IEEE Trans. Autom. Control*, vol. 40, no. 6, pp. 1083–1087, Jun. 1995.

[12] J. Zhou, C. Zhang, and C. Wen, "Robust adaptive output control of uncertain nonlinear plants with unknown backlash nonlinearity," *IEEE Trans. Autom. Control*, vol. 52, no. 3, pp. 503–509, Mar. 2007.

[13] W. He, X. He, M. Zou, and H. Li, "PDE model-based boundary control design for a flexible robotic manipulator with input backlash," *IEEE Trans. Control Syst. Technol.*, vol. 27, no. 2, pp. 790–797, Mar. 2019.

[14] L. Tang, X.-Y. Zhang, Y.-J. Liu, and S. Tong, "PDE based adaptive control of flexible riser system with input backlash and state constraints," *IEEE Trans. Circuits Syst. I, Reg. Papers*, vol. 69, no. 5, pp. 2193–2202, May 2022.

[15] X. He, Z. Zhao, J. Su, Q. Yang, and D. Zhu, "Adaptive inverse control of a vibrating coupled vessel-riser system with input backlash," *IEEE Trans. Syst., Man, Cybern., Syst.*, vol. 51, no. 8, pp. 4706–4715, Aug. 2021.

[16] J. Zhang, Y. Liu, Z. Zhao, T. Zou, and K.-S. Hong, "Vibration control for a nonlinear three-dimensional suspension cable with input and output constraints," *IEEE Trans. Syst., Man, Cybern., Syst.*, vol. 52, no. 12, pp. 7821–7832, Dec. 2022.

[17] Y. Yan, H. Zhang, Y. Mu, and J. Sun, "Fault-tolerant fuzzy-resilient control for fractional-order stochastic underactuated system with unmodeled dynamics and actuator saturation," *IEEE Trans. Cybern.*, early access, Jun. 1, 2023, doi: 10.1109/TCYB.2023.3273848.

[18] H. Deng, Y. Zhao, A.-T. Nguyen, and C. Huang, "Fault-tolerant predictive control with deep-reinforcement-learning-based torque distribution for four in-wheel motor drive electric vehicles," *IEEE/ASME Trans. Mechatronics*, vol. 28, no. 2, pp. 668–680, Apr. 2023.

[19] M. Hashemi, J. Askari, and J. Ghaisari, "Adaptive actuator failure compensation for a class of MIMO nonlinear time delay systems," *Nonlinear Dyn.*, vol. 79, no. 2, pp. 865–883, 2015.

[20] N. Ji, J. Liu, and H. Yang, "Boundary vibration suppression for a flexible three-dimensional marine riser against unknown sensor and actuator faults," *Int. J. Robust Nonlinear Control*, vol. 31, no. 5, pp. 1438–1451, 2021.

[21] Z. Zhao, Y. Ren, C. Mu, T. Zou, and K.-S. Hong, "Adaptive neural-network-based fault-tolerant control for a flexible string with composite disturbance observer and input constraints," *IEEE Trans. Cybern.*, vol. 52, no. 12, pp. 12843–12853, Dec. 2022.

[22] J.-W. Wang, Y.-Q. Liu, and C.-Y. Sun, "Adaptive neural boundary control design for nonlinear flexible distributed parameter systems," *IEEE Trans. Control Syst. Technol.*, vol. 27, no. 5, pp. 2085–2099, Sep. 2019.

[23] X. Xing and J. Liu, "Robust adaptive control allocation for a class of cascade ODE-string systems with actuator failures," *IEEE Trans. Autom. Control*, vol. 67, no. 3, pp. 1474–1481, Mar. 2022.

[24] G. Ma, Z. Tan, Y. Liu, Z. Zhao, and T. Zou, "Adaptive robust barrier-based control of a 3D flexible riser system subject to boundary displacement constraints," *Int. J. Robust Nonlinear Control*, vol. 32, no. 5, pp. 3062–3077, 2022.

[25] Z. Zhao, Y. Liu, T. Zou, K.-S. Hong, and H.-X. Li, "Robust adaptive fault-tolerant control for a riser-vessel system with input hysteresis and time-varying output constraints," *IEEE Trans. Cybern.*, vol. 53, no. 6, pp. 3939–3950, Jun. 2023.

[26] M. Wan, Y. Yin, J. Liu, and X. Guo, "Active boundary control of vibrating marine riser with constrained input in three-dimensional space," *Nonlinear Dyn.*, vol. 106, no. 3, pp. 2329–2345, 2021.

[27] J. Zhou and C. Wen, *Adaptive Backstepping Control of Uncertain Systems: Nonsmooth Nonlinearities, Interactions or Time-Variations*. Berlin, Germany: Springer, 2008.

[28] W. He, C. Sun, and S. S. Ge, "Top tension control of a flexible marine riser by using integral-barrier Lyapunov function," *IEEE/ASME Trans. Mechatronics*, vol. 20, no. 2, pp. 497–505, Apr. 2015.

[29] Z. Zhao, X. He, and G. Wen, "Boundary robust adaptive anti-saturation control of vibrating flexible riser systems," *Ocean Eng.*, vol. 179, pp. 298–306, May 2019.

[30] Y.-H. Jing and G.-H. Yang, "Adaptive quantised fault-tolerant tracking control of uncertain nonlinear systems with unknown control direction and the prescribed accuracy," *Int. J. Syst. Sci.*, vol. 48, no. 13, pp. 2826–2837, 2017.

[31] K. D. Do and J. Pan, "Boundary control of three-dimensional inextensible marine risers," *J. Sound Vib.*, vol. 327, nos. 3–5, pp. 299–321, 2009.

[32] Y. Ma, X. He, S. Zhang, Y. Sun, and Q. Fu, "Adaptive compensation for infinite number of actuator faults and time-varying delay of a flexible manipulator system," *IEEE Trans. Ind. Electron.*, vol. 69, no. 12, pp. 13141–13150, Dec. 2022.

[33] C. Yang, R. Chen, W. Wang, Y. Li, X. Shen, and C. Xiang, "Cyber-physical optimization-based fuzzy control strategy for plug-in hybrid electric buses using iterative modified particle swarm optimization," *IEEE Trans. Intell. Veh.*, vol. 8, no. 5, pp. 3285–3298, May 2023.

[34] J. Wang, Z. Liu, Y. Zhang, and C. L. P. Chen, "A novel fuzzy control with filter-based event-triggered mechanism for nonlinear uncertain stochastic systems suffered input hysteresis," *Fuzzy Sets Syst.*, vol. 432, pp. 68–88, Mar. 2022.

[35] Y.-X. Li and G.-H. Yang, "Adaptive asymptotic tracking control of uncertain nonlinear systems with input quantization and actuator faults," *Automatica*, vol. 72, pp. 177–185, Oct. 2016.

[36] M. Krstic, I. Kanellakopoulos, and P. V. Kokotovic, *Nonlinear and Adaptive Control Design*. New York, NY, USA: Wiley, 1995.

[37] Z. Jing, Y. Ma, X. Wu, X. He, and Y. Sun, "Backstepping control for vibration suppression of 2-D Euler–Bernoulli beam based on nonlinear saturation compensator," *IEEE Trans. Syst., Man, Cybern., Syst.*, vol. 53, no. 5, pp. 2562–2571, May 2023.

[38] S. Zhang, X. He, and C. Yang, "Vibration control of a flexible marine riser with joint angle constraint," *Nonlinear Dyn.*, vol. 87, pp. 617–632, Jan. 2017.

[39] L. Xing, C. Wen, Z. Liu, H. Su, and J. Cai, "Adaptive compensation for actuator failures with event-triggered input," *Automatica*, vol. 85, pp. 129–136, Nov. 2017.

[40] M. Hashemi, J. Askari, J. Ghaisari, and M. Kamali, "Robust adaptive actuator failure compensation for a class of uncertain nonlinear systems," *Int. J. Autom. Comput.*, vol. 14, no. 6, pp. 719–728, 2017.

[41] W. Wang, C. Wen, J. Huang, and J. Zhou, "Adaptive consensus of uncertain nonlinear systems with event triggered communication and intermittent actuator faults," *Automatica*, vol. 111, Jan. 2020, Art. no. 108667.

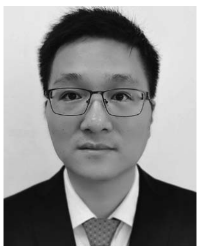

Zhijia Zhao (Member, IEEE) received the B.Eng. degree in automatic control from the North China University of Water Resources and Electric Power, Zhengzhou, China, in 2010, and the M.Eng. and Ph.D. degrees in automatic control from the South China University of Technology, Guangzhou, China, in 2013 and 2017, respectively.

He is currently an Associate Professor with the School of Mechanical and Electrical Engineering, Guangzhou University, Guangzhou. His research interests include adaptive and learning control, flexible mechanical systems, and robotics.

Yiming Liu received the B.Eng. degree in robotics engineering from Guangzhou University, Guangzhou, China, in 2021, where he is currently pursuing the master's degree in control science and engineering.

His research interests include flexible systems, distributed parameter system control, and robotics.

Ge Ma received the B.S. degree in information and computing science from Shandong Jianzhu University, Jinan, China, in 2010, and the Ph.D. degree in automatic control from the South China University of Technology, Guangzhou, China, in 2016.

She is currently a Lecturer with Guangzhou University, Guangzhou. Her research interests include computer vision, robotics, and automatic control.

Keum-Shik Hong (Fellow, IEEE) received the B.S. degree in mechanical design from Seoul National University, Seoul, South Korea, in 1979, the M.S. degree in mechanical engineering from Columbia University, New York, NY, USA, in 1987, and the M.E. degree in applied mathematics and the Ph.D. degree in mechanical engineering from the University of Illinois at Urbana–Champaign, Champaign, IL, USA, in 1991 and 1997, respectively.

He joined the School of Mechanical Engineering, Pusan National University, Busan, South Korea, in 1993. His research interests include brain–computer interface, nonlinear systems theory, adaptive control, and distributed parameter systems.

Dr. Hong has received many awards, including the Best Paper Award from the KFSTS of Korea in 1999 and the Presidential Award of Korea in 2007. He served as an Associate Editor for *Automatica* from 2000 to 2006 and the Editor-in-Chief for the *Journal of Mechanical Science and Technology* from 2008 to 2011, and serving as the Editor-in-Chief for the *International Journal of Control, Automation, and Systems*. He was the past President of the Institute of Control, Robotics and Systems (ICROS), South Korea, and the President of the Asian Control Association. He is a Fellow of the Korean Academy of Science and Technology, an ICROS Fellow, and a member of the National Academy of Engineering of Korea.

Han-Xiong Li (Fellow, IEEE) received the B.E. degree in aerospace engineering from the National University of Defense Technology, Changsha, China, in 1982, the M.E. degree in electrical engineering from the Delft University of Technology, Delft, The Netherlands, in 1991, and the Ph.D. degree in electrical engineering from the University of Auckland, Auckland, New Zealand, in 1997.

He is currently a Chair Professor with the Department of SEEM, City University of Hong Kong, Hong Kong. He has a broad experience in both academia and industry. He has authored two books and about 20 patents and has published more than 200 SCI journal articles with H-index 55 (Web of Science). His current research interests include process modeling and control, system intelligence, distributed parameter systems, and battery management systems.

Dr. Li was awarded the Distinguished Young Scholar (overseas) by the China National Science Foundation in 2004, a Chang Jiang Professorship by the Ministry of Education, China, in 2006, and a National Professorship in China Thousand Talents Program in 2010. He serves as a Distinguished Expert for Hunan Government and China Federation of Returned Overseas Chinese. He serves as an Associate Editor for IEEE TRANSACTIONS ON SYSTEMS, MAN, AND CYBERNETICS: SYSTEMS and was an Associate Editor of IEEE Transactions on Cybernetics from 2002 to 2016 and IEEE TRANSACTIONS ON INDUSTRIAL ELECTRONICS from 2009 to 2015.